Experimental Neurology 316 (2019) 63–73

Contents lists available at ScienceDirect

Experimental Neurology

journal homepage: www.elsevier.com/locate/yexnr

Research paper

Detection of brain specific cardiolipins in plasma after experimental pediatric head injury

Tamil S. Anthonymuthu[a,b,c,d,1], Elizabeth M. Kenny[a,b,c,d,1], Zachary E. Hier[a,b,c,d], Robert S.B. Clark[a,b], Patrick M. Kochanek[a,b], Valerian E. Kagan[d,e,f], Hülya Bayır[a,b,c,d,e,*]

[a] Department of Critical Care Medicine, University of Pittsburgh, Pittsburgh, PA, USA
[b] Safar Center for Resuscitation Research, University of Pittsburgh, Pittsburgh, PA, USA
[c] Center for Free Radical and Antioxidant Health, University of Pittsburgh, Pittsburgh, PA, USA
[d] Children's Neuroscience Institute, Children's Hospital of Pittsburgh, Pittsburgh, PA, USA
[e] Department of Environmental and Occupational Health, University of Pittsburgh, Pittsburgh, PA, USA
[f] Laboratory of Navigational Redox Lipidomics, IM Sechenov Moscow Medical State University, Russia

ARTICLE INFO

Keywords:
Mitochondrial dysfunction
Plasma biomarker
Brain-specific cardiolipin
Phospholipidomics

ABSTRACT

Cardiolipin (CL) is a mitochondria-specific phospholipid that is central to maintenance and regulation of mitochondrial bioenergetic and metabolic functions. CL molecular species display great tissue variation with brain exhibiting a distinct, highly diverse CL population. We recently showed that the appearance of unique brain-type CLs in plasma could serve as a brain-specific marker of mitochondrial/tissue injury in patients after cardiac arrest. Mitochondrial dysfunction has been increasingly implicated as a critical mechanism underlying the pathogenesis of traumatic brain injury (TBI). Therefore, we hypothesized that unique, brain-specific CL species from the injured brain are released to the peripheral circulation after TBI. To test this hypothesis, we performed a high-resolution mass spectrometry based phospholipidomics analysis of post-natal day (PND)17 rat brain and plasma after controlled cortical impact. We found a time-dependent increase in plasma CLs after TBI including the aforementioned brain-specific CL species early after injury, whereas CLs were significantly decreased in the injured brain. Compositional and quantitative correlational analysis suggested a possible release of CL into the systemic circulation following TBI. The identification of brain-type CLs in systemic circulation may indicate underlying mitochondrial dysfunction/loss after TBI. They may have potential as pharmacodynamics response biomarkers for targeted therapies.

1. Introduction

Traumatic brain injury (TBI) is the major cause of injury-associated morbidity and mortality among children under 14 years of age. TBI affects > 3 million children each year worldwide and about half a million children in the United States alone (Dewan et al., 2016). While the majority of childhood TBIs are mild, about 16% of TBI-related hospitalizations of adolescents are categorized as severe (Asemota et al., 2013). Recent developments in the therapeutic strategies and neurosurgical interventions (Kochanek et al., 2012) vastly reduced the mortality following severe pediatric TBI (Tilford et al., 2005). However nearly half of the severely injured TBI patients fail to achieve good to full functional recovery. In addition to long-term physical and cognitive debilitation in survivors of childhood TBI, there are also significant monetary and psychosocial burdens (Tilford et al., 2005).

Traumatic brain injury is a complex disease process, which consists of primary and secondary injury mechanisms. The primary injury is caused by the mechanical damage at the site of impact. Secondary injury is a progressive sequence of cellular events (Anthonymuthu et al., 2018). Mitochondria have been a focal point in the secondary injury effects of TBI (Robertson et al., 2009; Singh et al., 2006). Mitochondrial dysfunction and metabolic changes are seen as early as 30 min after TBI lasting up to 7 days (Singh et al., 2006). Multiple mitochondria-related events are observed such as aberrant calcium homeostasis, reduction in adenosine triphosphate (ATP) levels (Robertson et al., 2009), alteration in redox state (Stovell et al., 2018), uncoupling of oxidative phosphorylation (Kilbaugh et al., 2016) release of mitochondrial cytochrome *c* (Ji et al., 2012), and mitochondria-mediated cell death

* Corresponding author at: Center for Free Radical and Antioxidant Health, Safar Center for Resuscitation Research, University of Pittsburgh, USA.
E-mail address: bayihx@ccm.upmc.edu (H. Bayır).
[1] These authors contributed equally.

https://doi.org/10.1016/j.expneurol.2019.04.007
Received 20 December 2018; Received in revised form 14 March 2019; Accepted 10 April 2019
Available online 11 April 2019
0014-4886/

pathways such as apoptosis and necroptosis (Ji et al., 2012; You et al., 2008) after TBI. Therapies targeting mitochondrial metabolic changes and apoptosis have been shown to improve functional outcome after TBI in the developing brain (Ji et al., 2012; Robertson and Saraswati, 2015).

Glycerophospholipid cardiolipin (CL) is essential for the structural organization and function of mitochondria and is confined to the inner mitochondrial membrane (Kagan et al., 2015). As part of CL's role in structural organization, complexes III and IV destabilize in mitochondria lacking CL (Pfeiffer et al., 2003). CLs contain four fatty acyl chains resulting in the greatest structural diversity among all phospholipids. CLs can be remodeled by a post-synthetic pathway and each tissue displays varying levels of CL remodeling, resulting in tissue-specific CL spectra (Kagan et al., 2015). Brain tissue has a distinct CL profile based on the number of CL species, acyl chain lengths and degree of unsaturation (Kagan et al., 2015). We recently showed that the appearance of unique brain-type CLs in plasma could serve as a brain-specific marker of mitochondrial/tissue injury in adults after cardiac arrest (Anthonymuthu et al., 2019). Accumulation of three unique CL species [CL(70:3), CL(72:5) and CL(74,7)] correlated with neurological injury severity and functional outcome in these patients.

In addition to their structural roles, CLs play important signaling roles. Externalization of CL to the outer mitochondrial membrane acts as an “eat me” signal during mitophagy (Chu et al., 2013), whereas oxidation of CL is essential for execution of mitochondrial apoptosis (Kagan et al., 2005b). TBI triggers CL oxidation catalyzed by the intramembrane space hemoprotein, cytochrome *c*, and enzymatic hydrolysis of oxidized CL by calcium-independent phospholipase A2γ (iPLA2γ) (Liu et al., 2017) leading to formation of monolyso-CL and oxidized fatty acids as lipid mediators. This has specifically been shown to occur in the developing brain (Chao et al., 2018; Tyurina et al., 2014) after controlled cortical impact (CCI), CL content in the post-natal day (PND)17 rat brain decreases by ~60% compared to age-matched naïve animals (Chao et al., 2018). Quantitatively, the decrease in CL content is larger than expected considering the oxidation and hydrolysis of CL. Thus, it is likely that a portion of the mitochondrial CL is released into the interstitial space and subsequently into the circulation upon injury. In the current study, using high resolution liquid chromatography–mass spectrometry (LC-MS), we quantitatively assessed the temporal pattern of the brain and plasma CL profiles after CCI in PND17 rats to test the hypothesis that unique brain-type CL species will increase in plasma after CCI and that the increase in these species will quantitatively correlate with their loss from the injured cerebral cortex.

2. Materials and methods

2.1. Materials

All the solvents used in this study were either HPLC grade or LC-MS grade and obtained from Fisher Scientific USA. All the internal standards used were obtained from Avanti Polar Lipid Inc. Atlanta, USA.

2.2. Controlled cortical impact model and sample collection

The CCI model was performed as described previously (Bayir et al. 2007). Briefly, seventeen-day-old male Sprague–Dawley rats were anesthetized with 3.5% isoflurane in O_2. The trachea was intubated with a 14-gauge angiocatheter and rats were mechanically ventilated during sham and CCI surgery. Anesthesia was maintained with 2% isoflurane in N2O/O2 (2:1). and maintained on 2% isoflurane in N_2O/O_2 (2:1). A craniotomy was made over the left parietal cortex. For all studies, a 6-mm metal pneumatically driven impactor tip was used, velocity was 4.0 ± 0.2 m/s, depth of penetration was 2.5 mm, and duration of deformation was 50 milliseconds. After TBI, the bone flap was replaced, sealed with dental cement, and the scalp incision was closed. After a 1h monitoring period, rats were weaned from mechanical ventilation, extubated, and returned to their cages until further study. At euthanasia, plasma and cortex were collected and cortex was snap-frozen for lipidomics.

2.3. Lipid extraction and mass spectrometry analysis

The pericontusional cortex was isolated from the brain and the lipids were extracted using the folch method. Total phosphate content of the lipids was quantified using the method reported previously (Anthonymuthu et al., 2019). For phospholipid analysis, samples corresponding to approximately 2.5 nanomoles of total phosphate were supplemented with the appropriate internal standards (5 picomoles each of phosphatidylcholine (PC) (17:0/17:0), phosphatidylglycerol (PG) (17:0/17:0), phosphatidylinositol (PI) (16:0/16:0), CL (14:0/14:0/14:0/14:0), phosphatidylserine (PS) (17:0/17:0), phosphatidic acid (PA) (17:0/17:0), phosphatidylethanolamine (PE) (17,0/17:0)) and analyzed using LC-MS/MS. LC-MS/MS analysis was performed using a Dionex Ultimate 3000 RSLCnano system coupled on-line to a Q-Exactive hybrid quadrupole-orbitrap mass spectrometer (ThermoFisher Scientific, San Jose, CA) using a Silica column (Luna 3 µm, 100 Å, 150 × 2 mm, Phenomenex, Torrance CA). A multi-step gradient with solvents A (n-hexane/2-propanol/water/trimethylamine /formic acid, 43:57:1:0.5:0.01 *v*/v containing 10 mM ammonium acetate) and B (n-hexane/2-propanol/water/triethylamine/formic acid, 43:57:1:0.5:0.01 v/v containing 10 mM ammonium acetate) was used as follows: 0–15 min linear gradient from 10% B to 37% A at 200 µl/min, 15–23 min linear gradient from 37% to 40% B at 200 µl/min, 23–25 min linear gradient from 40% to 100% B and at a linear increase in flow rate at 200–225 µl/min, 27–47 min isocratic at 100% B at 225 µl/min, 47–57 min linear gradient from 100% to 10% B with a linear decrease in flow rate from 225 to 200 µl/min then the column was re-equilibrated for 13 min with 10% solvent B at 200 µl/min. The mass spectrum was acquired in a data-dependent acquisition with a negative ion mode from 0 to 57 min. The spray voltage was set as 3.2 KV with a sheath gas flow rate of 10 arbitrary units. The spectrum was recorded at 70000 FWHM resolution between 360 and 1600 *m/z* range with top 10 ions selected for fragmentation. HCD fragmentation with 24 NCE was used while the ions were isolated at +1 m/z isolation window.

Blood samples were centrifuged at 2000 × *g* for 15 min at 4 °C to collect plasma. The total lipids from plasma were extracted using the Bligh and Dyer method as described previously. Total phospholipid content was quantified using the micro method for phosphorus measurement (Anthonymuthu et al., 2019). Extracted lipids were re-suspended in n-hexane:2-propanol:water, 43:57:1 (*v*/v/v) and injected into liquid chromatography-tandem mass spectrometry (LC-MS/MS) system for lipid identification and quantification. Lipid extracts equivalent to 30 µl of plasma and 15 nmol of total phospholipids were used for CL and phospholipid analysis respectively. LC-MS/MS analysis was performed using a Dionex UltimateTM 3000 RSLCnano System coupled online to a Q-Exactive hybrid Quadrupole-Orbitrap mass spectrometer (ThermoFisher Scientific, San Jose, CA). Extracted lipids were injected into a normal phase column (Silica Luna 3 µm, 100 Å, 150 × 2 mm, Phenomenex, Torrance CA), and chromatography was performed using a gradient system of solvent A and solvent B (n-hexane:2-propanol:water, 43:57:8 [*v*/v/v]) with 10 mM ammonium acetate at the following intervals: 0–15 min, linear gradient of 10% to 37% B at 200 µl/min flow rate; 15–23 min, linear gradient of 65% B at 200 µl/min; 23–25 min, linear gradient of 100% B at 225 µl/min; 25–47 min, isocratic flow of 100% B at 225 µl/min; 47–57 min, linear gradient of 10% B at 200 µl/min; 57–70 min, re-equilibration of 10% B 200 µl/min for 15 min. Mass spectrometry was performed with the following conditions: Ion source-Heated Electron Spray Ionization, Spray voltage - 3.2 kV, capillary temperature- 320 °C, sheath gas flow-8 units, S-lens Rf level- 65. Mass spectra were collected at 140,000 full width at half maximum (FWHM) between 1220 and 1600 *m/z* and

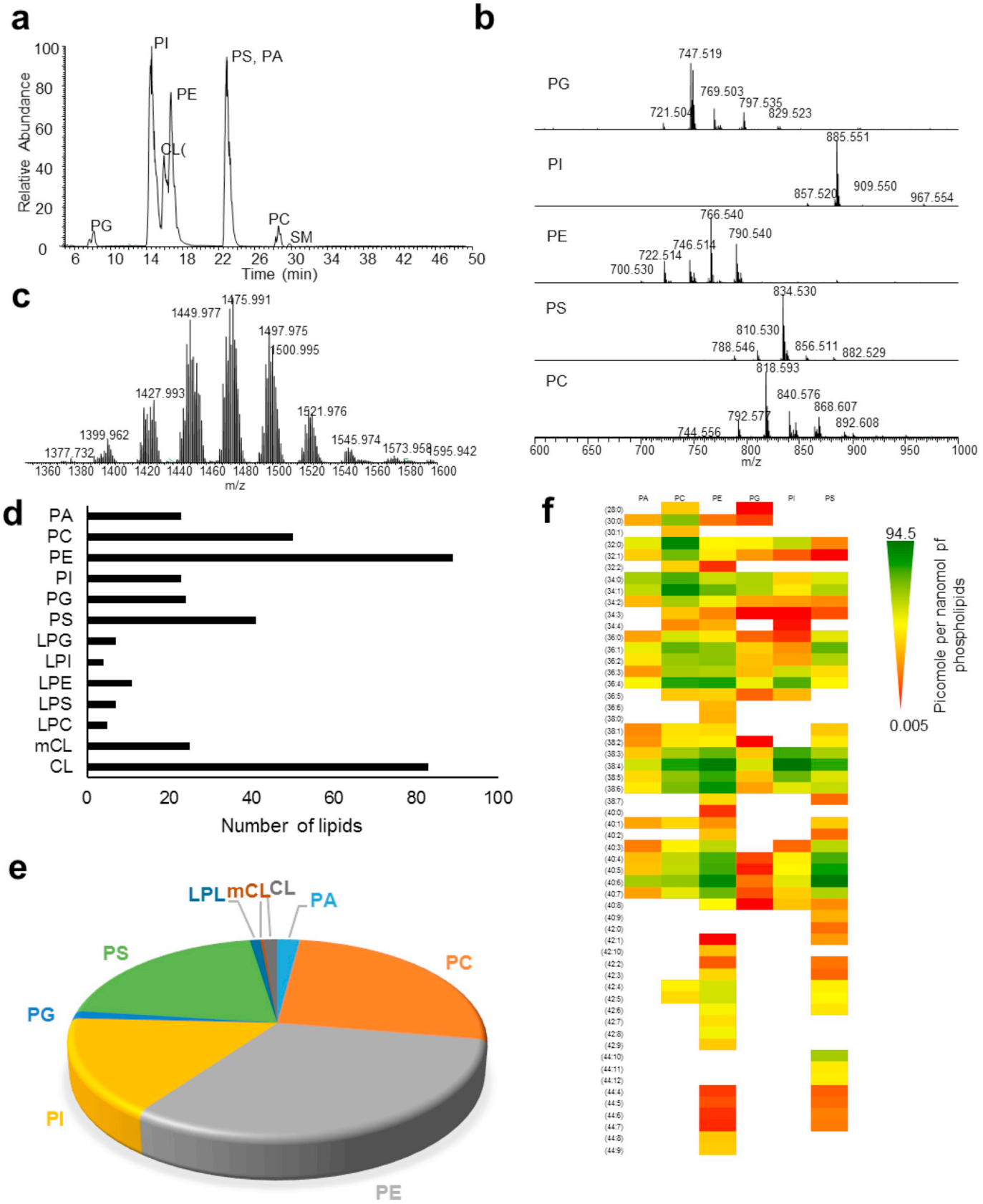

Fig. 1. Phospholipidome of pediatric rat brain. (A) Chromatogram of phospholipid classes from pediatric rat brain. Spectra showing different class of phospholipids (B) and cardiolipin (C). (D) Bar graph showing the number of species identified in each phospholipid class. (E) Pie chart showing the distribution of a given phospholipid quantity in each class. (F) Heat map showing the amount of different molecular species of major phospholipids except cardiolipin in the brain. PA: phosphatidic acid, PC: phosphatidylcholine, PE: phosphatidylethanolamine, PI: phosphatidylinositol, PG: phosphatidylglycerol, PS: phosphatidylserine, CL: cardiolipin, LPG: lyso-PG, LPI: lyso-PI, LPE: lyso-PE, LPS: lyso-PS, LPC: lyso-PC, mCL: monolyso-CL.

Table 1
Cardiolipin species identified in the PND17 rat brain.

Acyl carbons:Double bond	No PUFA	One PUFA	Two PUFA	Three PUFA	Four PUFA
66:6		$C_{14:0}C_{16:1}C_{16:1}C_{20:4}$	$C_{14:0}C_{14:0}C_{18:2}C_{20:4}$		
66:5		$C_{14:0}C_{14:0}C_{18:1}C_{20:4}$	$C_{14:0}C_{16:1}C_{18:2}C_{18:2}$		
		$C_{14:0}C_{16:0}C_{16:1}C_{20:4}$			
		$C_{16:1}C_{16:1}C_{16:1}C_{18:2}$			
66:4	$C_{16:1}C_{16:1}C_{16:1}C_{18:1}$	$C_{14:0}C_{16:1}C_{18:1}C_{18:2}$	$C_{14:0}C_{16:0}C_{18:2}C_{18:2}$		
		$C_{16:0}C_{16:1}C_{16:1}C_{18:2}$			
66:3	$C_{16:0}C_{16:1}C_{16:1}C_{18:1}$	$C_{16:0}C_{16:0}C_{16:1}C_{18:2}$			
	$C_{14:0}C_{16:1}C_{18:1}C_{18:1}$	$C_{14:0}C_{16:0}C_{18:1}C_{18:2}$			
66:2	$C_{14:0}C_{14:0}C_{18:1}C_{20:1}$	$C_{16:0}C_{16:0}C_{16:0}C_{18:2}$			
	$C_{14:0}C_{16:0}C_{16:1}C_{20:1}$				
	$C_{14:0}C_{16:0}C_{18:1}C_{18:1}$				
	$C_{16:0}C_{16:0}C_{16:1}C_{18:1}$				
68:7		$C_{16:1}C_{16:1}C_{16:1}C_{20:4}$	$C_{14:0}C_{16:1}C_{18:2}C_{20:4}$		
68:6		$C_{16:1}C_{16:1}C_{16:1}C_{20:3}$	$C_{16:1}C_{16:1}C_{18:2}C_{18:2}$	$C_{14:0}C_{18:2}C_{18:2}C_{18:2}$	
		$C_{16:0}C_{16:1}C_{16:1}C_{20:4}$	$C_{14:0}C_{16:1}C_{18:2}C_{20:3}$		
		$C_{14:0}C_{16:1}C_{18:1}C_{20:4}$	$C_{14:0}C_{16:0}C_{18:2}C_{20:4}$		
			$C_{14:0}C_{14:0}C_{20:3}C_{20:3}$		
68:5		$C_{16:1}C_{16:1}C_{18:1}C_{18:2}$	$C_{14:0}C_{18:1}C_{18:2}C_{18:2}$		
		$C_{14:0}C_{16:1}C_{18:1}C_{20:3}$			
		$C_{14:0}C_{16:1}C_{18:0}C_{20:4}$			
68:4	$C_{16:1}C_{16:1}C_{18:1}C_{18:1}$	$C_{16:0}C_{16:1}C_{18:1}C_{18:2}$	$C_{16:0}C_{16:0}C_{18:2}C_{18:2}$		
		$C_{16:0}C_{16:0}C_{16:1}C_{20:3}$			
		$C_{14:0}C_{18:1}C_{18:1}C_{18:2}$			
		$C_{14:0}C_{16:0}C_{18:1}C_{20:3}$			
		$C_{16:0}C_{16:0}C_{16:0}C_{20:4}$			
68:3	$C_{16:0}C_{16:1}C_{18:1}C_{18:1}$	$C_{16:0}C_{16:0}C_{18:1}C_{18:2}$			
68:2	$C_{16:0}C_{16:0}C_{18:1}C_{18:1}$				
70:10		$C_{16:1}C_{16:2}C_{18:1}C_{20:6}$	$C_{16:1}C_{16:1}C_{18:2}C_{20:6}$		$C_{16:2}C_{16:2}C_{18:2}C_{20:4}$
70:8		$C_{14:0}C_{16:1}C_{18:1}C_{22:6}$	$C_{14:0}C_{16:0}C_{18:2}C_{22:6}$	$C_{14:0}C_{18:2}C_{18:2}C_{20:4}$	
		$C_{16:0}C_{16:1}C_{16:1}C_{22:6}$	$C_{14:0}C_{16:0}C_{20:4}C_{20:4}$		
			$C_{16:1}C_{16:1}C_{18:2}C_{20:4}$		
70:7		$C_{16:1}C_{16:1}C_{18:1}C_{20:4}$	$C_{14:0}C_{18:1}C_{18:2}C_{20:4}$	$C_{16:1}C_{18:2}C_{18:2}C_{18:2}$	
			$C_{16:0}C_{16:1}C_{18:2}C_{20:4}$		
70:6		$C_{16:0}C_{16:1}C_{18:1}C_{20:4}$	$C_{16:1}C_{18:1}C_{18:2}C_{18:2}$	$C_{16:0}C_{18:2}C_{18:2}C_{18:2}$	
		$C_{14:0}C_{18:1}C_{18:1}C_{20:4}$	$C_{16:0}C_{16:0}C_{18:2}C_{20:4}$		
70:5	$C_{16:1}C_{16:1}C_{18:2}C_{20:1}$	$C_{16:0}C_{16:1}C_{18:1}C_{20:3}$	$C_{16:0}C_{16:0}C_{18:2}C_{20:3}$		
70:5		$C_{16:1}C_{18:1}C_{18:1}C_{18:2}$	$C_{16:0}C_{18:1}C_{18:2}C_{18:2}$		
		$C_{14:0}C_{16:1}C_{20:3}C_{20:1}$	$C_{14:0}C_{18:2}C_{18:2}C_{20:1}$		
		$C_{16:0}C_{16:0}C_{18:1}C_{20:4}$			
		$C_{14:0}C_{16:0}C_{20:4}C_{20:1}$			
		$C_{14:0}C_{18:1}C_{18:1}C_{20:3}$			
70:4	$C_{16:1}C_{18:1}C_{18:1}C_{18:1}$	$C_{16:1}C_{18:0}C_{18:1}C_{18:2}$	$C_{16:0}C_{18:0}C_{18:2}C_{18:2}$		
		$C_{16:0}C_{18:1}C_{18:1}C_{18:2}$			
		$C_{14:0}C_{18:0}C_{18:0}C_{20:4}$			
		$C_{16:0}C_{16:0}C_{18:0}C_{20:4}$			
70:3	$C_{16:0}C_{18:1}C_{18:1}C_{18:1}$				
70:2	$C_{16:1}C_{18:0}C_{18:0}C_{18:1}$				
	$C_{16:0}C_{18:0}C_{18:1}C_{18:1}$				
72:10			$C_{16:1}C_{16:1}C_{18:2}C_{22:6}$		
			$C_{16:1}C_{16:1}C_{20:4}C_{20:4}$		
72:9		$C_{16:1}C_{16:1}C_{18:1}C_{22:6}$	$C_{14:0}C_{16:0}C_{20:3}C_{22:6}$		
			$C_{14:0}C_{18:1}C_{18:2}C_{22:6}$	$C_{14:0}C_{18:2}C_{20:4}C_{20:3}$	
			$C_{14:0}C_{18:1}C_{20:4}C_{20:4}$	$C_{16:1}C_{18:2}C_{18:2}C_{20:4}$	
			$C_{16:1}C_{16:1}C_{20:4}C_{20:3}$		
			$C_{16:0}C_{16:1}C_{18:2}C_{22:6}$		
			$C_{16:0}C_{16:1}C_{20:4}C_{20:4}$		
72:8		$C_{16:0}C_{16:1}C_{18:1}C_{22:6}$	$C_{16:1}C_{18:1}C_{18:2}C_{20:4}$	$C_{16:0}C_{18:2}C_{18:2}C_{20:4}$	$C_{18:2}C_{18:2}C_{18:2}C_{18:2}$
		$C_{14:0}C_{18:1}C_{18:1}C_{22:6}$	$C_{16:0}C_{16:0}C_{18:2}C_{22:6}$		
			$C_{16:0}C_{16:0}C_{20:4}C_{20:4}$		
72:7		$C_{16:1}C_{18:1}C_{18:1}C_{20:4}$	$C_{16:0}C_{16:1}C_{20:3}C_{20:3}$	$C_{16:0}C_{18:2}C_{18:2}C_{20:3}$	
			$C_{16:1}C_{18:1}C_{18:2}C_{20:3}$	$C_{18:1}C_{18:2}C_{18:2}C_{18:2}$	
			$C_{16:1}C_{18:0}C_{18:2}C_{20:4}$		
			$C_{16:0}C_{16:0}C_{20:4}C_{20:3}$		
			$C_{16:0}C_{18:1}C_{18:2}C_{20:4}$		
			$C_{14:0}C_{18:1}C_{20:3}C_{20:3}$		
			$C_{14:0}C_{18:0}C_{20:4}C_{20:3}$		
72:6		$C_{16:1}C_{18:1}C_{18:1}C_{20:3}$	$C_{16:1}C_{18:0}C_{18:2}C_{20:3}$	$C_{18:0}C_{18:2}C_{18:2}C_{18:2}$	
		$C_{16:1}C_{18:0}C_{18:1}C_{20:4}$	$C_{18:1}C_{18:1}C_{18:2}C_{18:2}$		
		$C_{16:0}C_{18:1}C_{18:1}C_{20:4}$	$C_{16:0}C_{18:1}C_{18:2}C_{20:3}$		
			$C_{16:0}C_{18:0}C_{18:2}C_{20:4}$		
			$C_{16:0}C_{16:0}C_{20:3}C_{20:3}$		
72:5		$C_{16:1}C_{18:0}C_{18:0}C_{20:4}$	$C_{18:0}C_{18:1}C_{18:2}C_{18:2}$		
		$C_{18:1}C_{18:1}C_{18:1}C_{18:2}$			
		$C_{16:0}C_{18:0}C_{18:1}C_{20:4}$			

(*continued on next page*)

Table 1 (*continued*)

Acyl carbons:Double bond	No PUFA	One PUFA	Two PUFA	Three PUFA	Four PUFA
72:4	$C_{18:1}C_{18:1}C_{18:1}C_{18:1}$	$C_{18:0}C_{18:1}C_{18:1}C_{18:2}$ $C_{16:0}C_{16:0}C_{18:2}C_{22:2}$ $C_{16:0}C_{18:0}C_{18:0}C_{20:4}$	$C_{18:0}C_{18:0}C_{18:2}C_{18:2}$		
72:3	$C_{18:0}C_{18:1}C_{18:1}C_{18:1}$				
72:2	$C_{18:0}C_{18:0}C_{18:1}C_{18:1}$	$C_{18:0}C_{18:0}C_{18:0}C_{18:2}$			
74:11			$C_{16:1}C_{16:1}C_{20:4}C_{22:5}$ $C_{16:1}C_{16:1}C_{20:3}C_{22:6}$ $C_{14:0}C_{16:1}C_{22:5}C_{22:5}$ $C_{14:0}C_{20:4}C_{20:4}C_{20:3}$ $C_{14:0}C_{18:1}C_{20:4}C_{22:6}$	$C_{16:1}C_{18:2}C_{18:2}C_{22:6}$ $C_{16:1}C_{18:2}C_{20:4}C_{20:4}$ $C_{14:0}C_{18:2}C_{20:4}C_{22:5}$ $C_{14:0}C_{18:2}C_{20:3}C_{22:6}$	
74:10			$C_{16:1}C_{18:1}C_{18:2}C_{22:6}$ $C_{16:1}C_{18:1}C_{20:4}C_{20:4}$ $C_{16:0}C_{16:0}C_{20:4}C_{22:6}$	$C_{16:1}C_{18:2}C_{20:4}C_{20:3}$ $C_{16:0}C_{16:1}C_{20:3}C_{22:6}$ $C_{16:0}C_{18:2}C_{18:2}C_{22:6}$ $C_{16:0}C_{18:2}C_{20:4}C_{20:4}$	$C_{18:2}C_{18:2}C_{18:2}C_{20:4}$
74:9		$C_{16:1}C_{18:1}C_{18:1}C_{22:6}$ $C_{18:1}C_{18:1}C_{18:1}C_{20:4}$	$C_{16:1}C_{18:1}C_{20:4}C_{20:3}$ $C_{16:0}C_{18:1}C_{18:2}C_{22:6}$ $C_{16:0}C_{18:1}C_{20:4}C_{20:4}$ $C_{16:0}C_{16:0}C_{20:3}C_{22:6}$	$C_{16:1}C_{18:2}C_{20:3}C_{20:3}$ $C_{18:1}C_{18:2}C_{18:2}C_{20:4}$ $C_{16:0}C_{18:2}C_{20:4}C_{20:3}$	$C_{18:2}C_{18:2}C_{18:2}C_{20:3}$
74:8			$C_{18:1}C_{18:1}C_{18:2}C_{20:4}$	$C_{16:1}C_{18:2}C_{20:2}C_{20:2}$	
74:7			$C_{16:1}C_{18:1}C_{20:3}C_{20:2}$ $C_{16:1}C_{18:0}C_{20:4}C_{20:2}$ $C_{16:1}C_{18:0}C_{20:3}C_{20:3}$ $C_{16:0}C_{18:2}C_{20:3}C_{20:2}$ $C_{16:0}C_{18:1}C_{20:4}C_{20:2}$ $C_{16:0}C_{18:1}C_{20:3}C_{20:3}$ $C_{16:0}C_{18:0}C_{20:4}C_{20:3}$ $C_{18:1}C_{18:1}C_{18:2}C_{20:3}$ $C_{18:0}C_{18:1}C_{18:2}C_{20:4}$	$C_{18:1}C_{18:2}C_{18:2}C_{20:2}$ $C_{18:0}C_{18:2}C_{18:2}C_{20:3}$	
74:6		$C_{16:0}C_{18:0}C_{18:0}C_{22:6}$ $C_{18:1}C_{18:1}C_{18:1}C_{20:3}$ $C_{18:0}C_{18:1}C_{18:1}C_{20:4}$	$C_{16:1}C_{18:1}C_{20:2}C_{20:2}$ $C_{16:1}C_{18:0}C_{20:3}C_{20:2}$ $C_{16:0}C_{18:1}C_{20:3}C_{20:2}$ $C_{16:0}C_{18:0}C_{20:4}C_{20:2}$ $C_{16:0}C_{18:0}C_{20:3}C_{20:3}$ $C_{18:1}C_{18:1}C_{18:2}C_{20:2}$ $C_{18:0}C_{18:0}C_{18:2}C_{20:4}$	$C_{16:0}C_{18:2}C_{20:2}C_{20:2}$ $C_{18:0}C_{18:2}C_{18:2}C_{20:2}$ $C_{18:0}C_{18:1}C_{18:2}C_{20:3}$	
74:5		$C_{18:0}C_{18:1}C_{18:1}C_{20:3}$ $C_{18:0}C_{18:0}C_{18:1}C_{20:4}$	$C_{18:0}C_{18:0}C_{18:2}C_{20:3}$		
74:4		$C_{18:0}C_{18:0}C_{18:1}C_{20:3}$ $C_{18:0}C_{18:0}C_{18:0}C_{20:4}$			
76:13			$C_{16:0}C_{16:1}C_{22:6}C_{22:6}$	$C_{16:1}C_{18:2}C_{20:4}C_{22:6}$ $C_{16:1}C_{20:4}C_{20:4}C_{20:4}$	
76:12			$C_{16:0}C_{16:0}C_{22:6}C_{22:6}$ $C_{16:1}C_{18:1}C_{20:3}C_{22:6}$	$C_{16:0}C_{20:4}C_{20:4}C_{20:4}$ $C_{16:1}C_{18:2}C_{20:2}C_{22:6}$	$C_{20:4}C_{20:3}C_{20:2}C_{16:2}$ $C_{20:3}C_{20:3}C_{20:3}C_{16:2}$
76:11			$C_{16:1}C_{18:0}C_{20:4}C_{22:6}$	$C_{16:1}C_{20:4}C_{20:4}C_{20:2}$ $C_{16:1}C_{20:4}C_{20:3}C_{20:3}$ $C_{18:1}C_{20:2}C_{22:6}C_{16:2}$ $C_{18:0}C_{20:3}C_{22:6}C_{16:2}$ $C_{18:1}C_{18:2}C_{18:2}C_{22:6}$ $C_{18:1}C_{18:2}C_{20:4}C_{20:4}$	$C_{18:2}C_{18:2}C_{20:4}C_{20:3}$
76:10			$C_{16:1}C_{18:1}C_{20:2}C_{22:6}$ $C_{16:1}C_{18:0}C_{20:3}C_{22:6}$ $C_{18:0}C_{20:2}C_{22:6}C_{16:2}$ $C_{18:1}C_{18:1}C_{18:2}C_{22:6}$ $C_{18:1}C_{18:1}C_{20:4}C_{20:4}$	$C_{16:1}C_{20:4}C_{20:3}C_{20:2}$ $C_{16:1}C_{20:3}C_{20:3}C_{20:3}$ $C_{18:0}C_{18:2}C_{18:2}C_{22:6}$ $C_{18:1}C_{18:2}C_{20:4}C_{20:3}$ $C_{18:0}C_{18:2}C_{20:4}C_{20:4}$	$C_{20:4}C_{20:2}C_{20:2}C_{16:2}$ $C_{20:3}C_{20:3}C_{20:2}C_{16:2}$ $C_{18:2}C_{18:2}C_{20:4}C_{20:2}$ $C_{18:2}C_{18:2}C_{20:3}C_{20:3}$
76:9		$C_{18:1}C_{18:1}C_{18:1}C_{22:6}$	$C_{16:0}C_{16:1}C_{22:4}C_{22:4}$ $C_{16:1}C_{18:1}C_{20:3}C_{22:4}$ $C_{16:0}C_{16:0}C_{22:5}C_{22:4}$ $C_{16:0}C_{18:1}C_{20:4}C_{22:4}$ $C_{16:0}C_{18:1}C_{20:3}C_{22:5}$ $C_{18:1}C_{18:1}C_{18:2}C_{22:5}$ $C_{18:1}C_{18:1}C_{20:4}C_{20:3}$	$C_{16:0}C_{18:2}C_{20:3}C_{22:4}$ $C_{16:0}C_{20:3}C_{20:3}C_{20:3}$ $C_{18:1}C_{18:2}C_{18:2}C_{22:4}$ $C_{18:1}C_{18:2}C_{20:3}C_{20:3}$	
76:8			$C_{18:1}C_{18:1}C_{20:3}C_{20:3}$	$C_{16:1}C_{20:2}C_{20:2}C_{20:2}$	
76:7			$C_{18:1}C_{18:2}C_{20:2}C_{20:2}$ $C_{18:1}C_{18:1}C_{20:3}C_{20:2}$		
78:14			$C_{16:1}C_{18:1}C_{22:6}C_{22:6}$	$C_{16:1}C_{18:2}C_{22:6}C_{22:5}$ $C_{16:1}C_{20:4}C_{20:4}C_{22:5}$ $C_{16:0}C_{18:2}C_{22:6}C_{22:6}$ $C_{16:0}C_{20:4}C_{20:4}C_{22:6}$	$C_{18:2}C_{18:2}C_{20:4}C_{22:6}$ $C_{18:2}C_{20:4}C_{20:4}C_{20:4}$

(*continued on next page*)

Table 1 (*continued*)

Acyl carbons:Double bond	No PUFA	One PUFA	Two PUFA	Three PUFA	Four PUFA
78:13			$C_{16:1}C_{18:1}C_{22:6}C_{22:5}$ $C_{16:1}C_{18:0}C_{22:6}C_{22:6}$ $C_{16:0}C_{18:1}C_{22:6}C_{22:6}$	$C_{16:1}C_{18:2}C_{22:5}C_{22:5}$ $C_{16:0}C_{18:2}C_{22:6}C_{22:5}$ $C_{16:0}C_{20:4}C_{20:4}C_{22:5}$ $C_{18:1}C_{18:2}C_{20:4}C_{22:6}$ $C_{18:1}C_{20:4}C_{20:4}C_{20:4}$	$C_{18:2}C_{18:2}C_{20:4}C_{22:5}$
78:12			$C_{18:1}C_{18:1}C_{20:4}C_{22:6}$	$C_{18:1}C_{18:2}C_{20:3}C_{22:6}$ $C_{18:0}C_{18:2}C_{20:4}C_{22:6}$ $C_{18:2}C_{20:4}C_{20:3}C_{20:3}$ $C_{18:1}C_{20:4}C_{20:4}C_{20:3}$ $C_{18:0}C_{20:4}C_{20:4}C_{20:4}$	$C_{18:2}C_{18:2}C_{20:4}C_{22:4}$
78:11			$C_{18:1}C_{18:1}C_{20:4}C_{22:5}$ $C_{18:1}C_{18:1}C_{20:3}C_{22:6}$ $C_{18:0}C_{18:1}C_{20:4}C_{22:6}$ $C_{18:0}C_{18:0}C_{22:5}C_{20:6}$	$C_{18:1}C_{18:2}C_{20:3}C_{22:5}$ $C_{18:0}C_{18:2}C_{20:4}C_{22:5}$ $C_{18:1}C_{20:4}C_{20:3}C_{20:3}$ $C_{16:1}C_{18:0}C_{22:5}C_{22:5}$ $C_{18:0}C_{20:4}C_{20:4}C_{20:3}$	$C_{18:2}C_{20:3}C_{20:3}C_{20:3}$ $C_{18:0}C_{18:2}C_{20:3}C_{22:6}$
78:10			$C_{18:1}C_{18:1}C_{20:4}C_{22:4}$	$C_{18:1}C_{18:2}C_{20:3}C_{22:4}$ $C_{18:1}C_{20:3}C_{20:3}C_{20:3}$	$C_{18:2}C_{18:2}C_{18:2}C_{24:4}$
78:9				$C_{18:1}C_{18:2}C_{20:2}C_{22:4}$ $C_{18:1}C_{18:1}C_{20:3}C_{22:4}$ $C_{18:1}C_{20:3}C_{20:3}C_{20:2}$	$C_{18:2}C_{20:3}C_{20:2}C_{20:2}$ $C_{18:1}C_{20:4}C_{20:2}C_{20:2}$
80:12			$C_{18:1}C_{18:1}C_{22:6}C_{22:4}$	$C_{18:1}C_{20:4}C_{20:3}C_{22:4}$ $C_{16:0}C_{20:4}C_{22:4}C_{22:4}$ $C_{16:1}C_{20:3}C_{22:4}C_{22:4}$	$C_{20:3}C_{20:3}C_{20:3}C_{20:3}$ $C_{18:2}C_{20:3}C_{20:3}C_{22:4}$ $C_{18:2}C_{18:2}C_{22:4}C_{22:4}$

300–1600 m/z respectively. Fragmentation was triggered in a data-dependent mode with top-5 intensity ions from the inclusion list isolated and fragmented by high collision dissociation (HCD) with a normalized collision energy (NCE) of 24.

2.4. Identification and quantification of lipid species

Identification and quantitation of the lipid species were performed with an optimized workflow developed for the redox lipidome using Compound discoverer v.2.0 software (ThermoFisher Scientific, San Jose, CA) as described earlier. In brief, the peaks with S/N ratio > 3 and minimum ion intensity of 5000 were identified and searched against phospholipid targeted *m/z* list generated for all possible acyl chain combinations of phospholipids. The list was further filtered by the retention time (RT) for each lipid class. Lipids eluted within 2.5 min of the internal standards retention time were considered for further analysis. The identified lipids were manually confirmed by verifying the fragmentation pattern of representative lipids of the same class. The values obtained were normalized to the internal standard and quantified using a calibration curve.

2.4.1. Data analysis and statistics

Most of the statistical analyses were performed using SPSS software (IBM Corporation, Armonk, NY). Orthogonal Projections to Latent Structures Discriminant Analysis (OPLS-DA) was performed using SIMCA (UMETRICS) software. A P value < .05 was considered a significant change.

3. Results

3.1. Phospholipidome of the PND17 rat brain

In order to determine the phospholipidome of the immature brain, we performed a high-resolution LC-MS/MS analysis of cortical tissue from PND17 rats. Phospholipids were separated based on their head group using a normal phase chromatography (Fig. 1A). The individual lipid species were identified based on exact mass and retention time (Fig. 1B). The identity of each lipid class was further confirmed by fragmentation analysis of representative species. We identified 392 isobaric phospholipid species in the immature naïve cortex (Fig. 1C). Phosphatidylethanolamine was the lipid class with the highest number (n = 89) of lipid species. This was followed by CL, PC, and PS with 83, 50 and 41 species in each class, respectively. Since a given isobaric mass may correspond to multiple individual molecular species of CL, we next performed fragmentation analysis to identify fatty acyl chains in each CL. Based on the fragmentation data of 51 isobaric CL species, we identified a total of 284 different CL species (Table 1). 272 of these species contained at least one oxidizable polyunsaturated fatty acid (PUFA). Quantitatively, 32% of cortical phospholipids consisted of PE followed by PC (26%), PS (21%) and PI (16%) (Fig. 1D). CL constituted about 1% of the total phospholipids. The brain phospholipidome showed a high dynamic range with the amounts of individual lipid species varying between 0.005 picomoles and 95 picomoles per nanomole of phospholipids (Fig. 1E). 1-stearoyl-2-arachidonoyl-sn-glycero-phosphoinositol was the most abundant lipid species which constituted 10.3% of the total phospholipid. This was followed by 1-stearoyl-2-docosahexaenoyl-sn-glycero-phosphoserine with 9.6% of the total phospholipids (Fig. 1F).

3.2. Changes in the brain phospholipidome after CCI

After defining the phospholipidome in the immature cortical tissue, we next analyzed the temporal course of its alterations after CCI in PND17 rats. As shown in Fig. 2, there was a significant change in the phospholipidome of the pericontusional cortex at 4 and 24 h after CCI. The most significant changes were observed in two classes of lipids, lysophospholipids, and CLs (Fig. 2). While the contents of lysophospholipids increased, CL levels decreased after injury. Among the lysophospholipids, the largest increase was observed in lysophosphatidylethanolamine (2-fold and 5-fold increase at 4 and 24 h, respectively) and lysophosphatidylcholine (1.7-fold and 5-fold increase at 4 and 24 h, respectively). The decrease in CL was nearly uniform across all identified species—approximately 96% and 89% of the identified species decreased at 4 and 24 h after CCI, respectively.

3.3. The phospholipidome of PND17 rat plasma

Using LC/MS we quantified 494 phospholipid species from all major classes in naïve PND17 rats plasma. PC dominated the plasma phospholipidome both in number of species and in quantity. PC accounted for 122 of the 494 spices and 77% of the total phospholipids in plasma. Quantitatively, PC (34:2) constituted 22% of the total phospholipids. PE was the second most abundant phospholipid class contributing up to 17% of the phospholipids (Fig. 1B). The number of PE molecular species

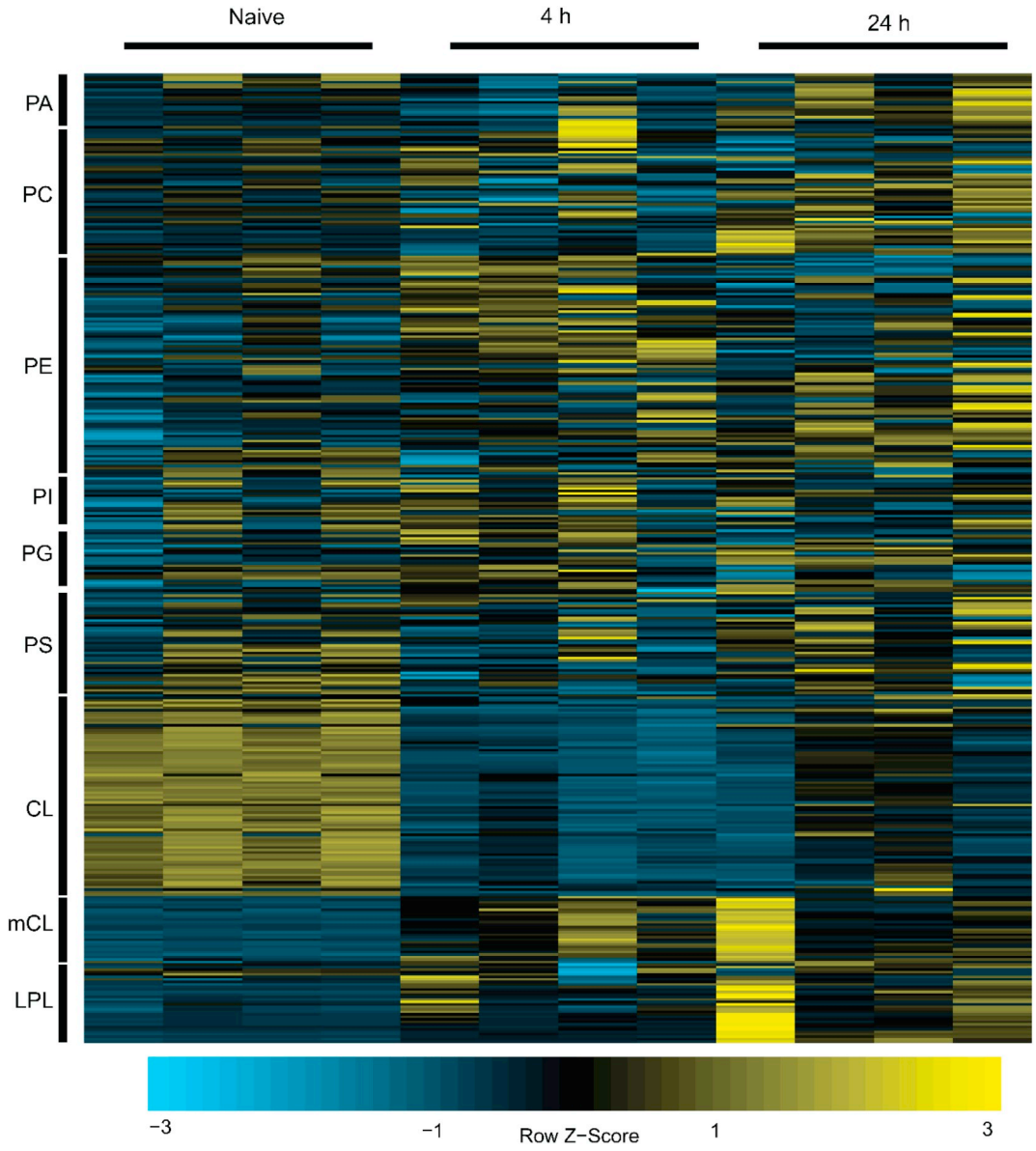

Fig. 2. Heat map showing the changes in the brain phospholipidome after CCI. Row *Z*-score depicts the normalized distribution of CL levels across all samples [Z-score = (Sample value – mean)/SD]. Z-score of 0 is marked by black cells and indicates that the sample value is identical to mean value. Z-score of +3 and − 3 are marked bright yellow and by bright blue cells and they indicate that the sample value is 3 standard deviations above or below the mean, respectively. Brain CL levels were lower at 4 h and 24 h while monolyso-CL and lyso-PL were higher at 4 h and 24 h after CCI vs. naïve. The lowest brain CLs levels were observed at 4 h after injury. (For interpretation of the references to colour in this figure legend, the reader is referred to the web version of this article.)

in the brain and plasma phospholipidomes was similar. Phosphatidic acid (PA) was among the less abundant phospholipid classes with just 7 species (Fig. 3A). As expected, CLs were the least abundant phospholipid class and could not be detected by the total phospholipid analysis method. Recently established targeted high-resolution LC/MS-MS analysis (Anthonymuthu et al., 2019), however, identified 90 CL species and showed that the total amount of CLs in the naïve plasma was < 0.001% of the total phospholipids (Fig. 3B).

3.4. Changes in plasma cardiolipinome after CCI

After establishing the phospholipidome of plasma from naive PND17 rats, we analyzed the changes in plasma phospholipidome after CCI. Multivariate analysis using OPLS-DA revealed that plasma phospholipidome was significantly different between naïve, 4 h and 24 h post CCI groups (Fig. 3C). Interestingly, all of the top 25 lipids with high variable influence on projection were CL species (Table 2). Notably, the majority of the species that were different between the naïve and CCI plasma were CL species that are uniquely enriched in the brain (Anthonymuthu et al., 2019; Kagan et al., 2015). Similar to adult cardiac arrest victims with neurological injury, PND17 rats showed increases in plasma CL(70:3) and CL(72:5) after CCI (Fig. 3D). There was a time-dependent progressive increase in plasma levels of brain-specific CLs after CCI (Fig. 3E).

3.5. The increase in plasma CL correlate with the decrease in brain CL after TBI

We then compared the brain CL species that decreased in ipsilateral cortex to the CL species that increased in the plasma at 24 h after CCI. The amounts of loss in brain CL and increase in plasma CL correlate significantly ($R = 0.56, p < .001$). As seen in the Fig. 4 all of the brain-

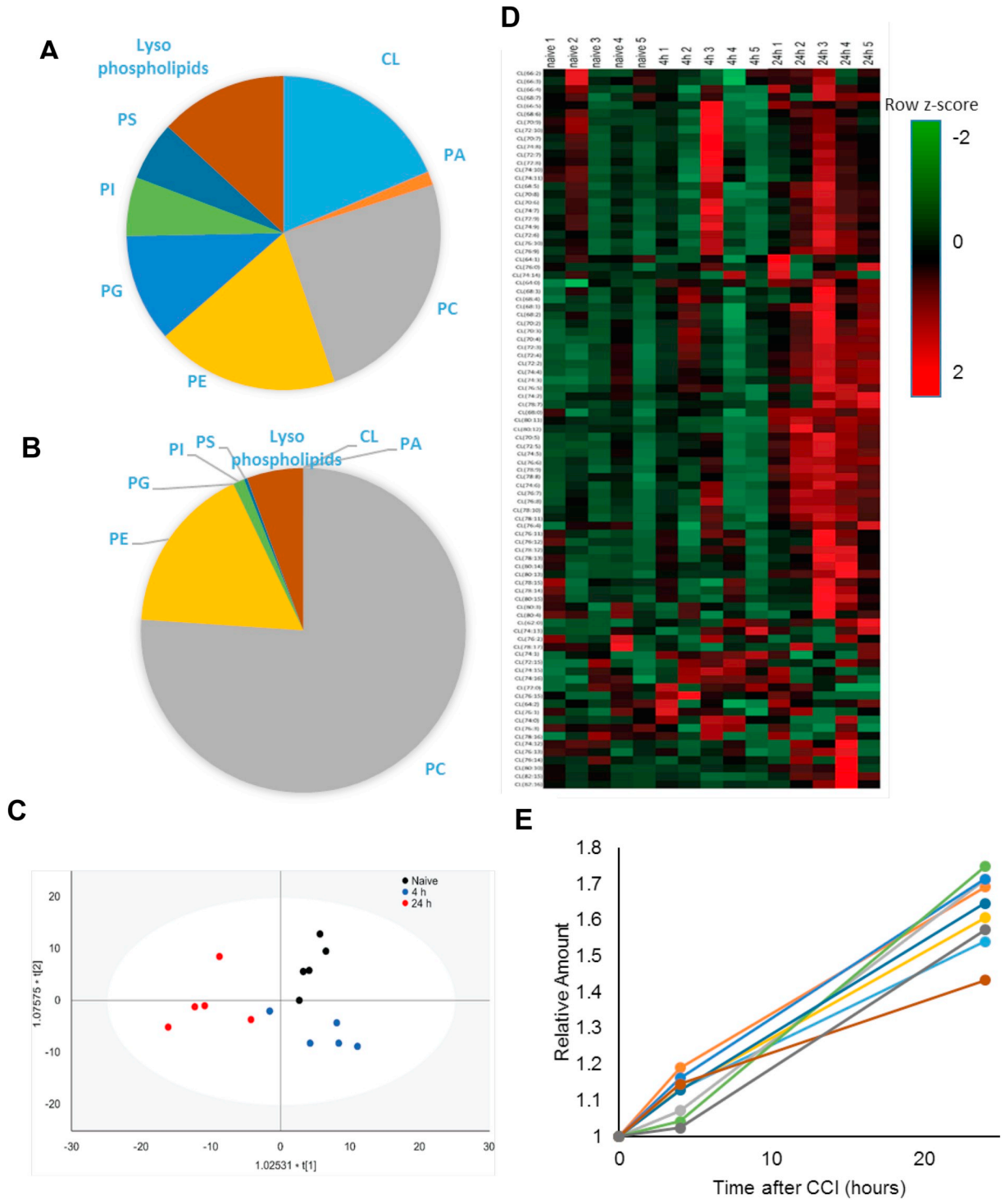

Fig. 3. Phospholipidome of PND17 rat plasma and its changes after traumatic brain injury. Pie charts showing the distribution of number (A) and amount (B) of phospholipid species in plasma. (C) Score plot of orthogonal value vs predictive value from the OPLS-DA model. D) Heat map showing the amount of different species of cardiolipins identified in plasma in naïve and TBI rats at 4 h and 24 h after injury. Individual species of CL are shown as CL(XX:YY), where XX represents total acyl carbons and YY represents total double bonds. Row Z-score depicts the normalized distribution of CL levels across all samples. [Z-score = (Sample value – mean)/SD]. Z-score of 0 is marked by black cells and indicates that the sample value is identical to mean value. Z-score of +2 and − 2 are marked bright red and by bright green cells and they indicate that the sample value is 2 standard deviations above or below the mean, respectively. E) Scatter line plot showing the temporal changes in brain-specific cardiolipins in plasma. (For interpretation of the references to colour in this figure legend, the reader is referred to the web version of this article.)

specific CL species were decreased in the injured cortex while increasing in the plasma. These results suggest a reciprocal relationship reflecting that part of the CL species lost from the cortical tissue appears in the plasma at 24 h after CCI.

4. Discussion

This is the first study showing that unique brain-type CL species increase in plasma after experimental pediatric TBI and the increase in these species quantitatively correlates with their loss from the injured

Table 2
List of top 25 lipids that differentiate CCI plasma phospholipidome.

Rank	Lipid	Variable importance for predictive components
1	CL(78:8)	1.84922
2	CL(76:6)	1.84446
3	CL(78:9)	1.83938
4	CL(78:10)	1.83871
5	CL(70:5)	1.8373
6	CL(72:5)	1.83331
7	CL(76:7)	1.81214
8	CL(78:11)	1.80009
9	CL(78:7)	1.80008
10	CL(74:5)	1.7983
11	CL(74:4)	1.79464
12	CL(74:3)	1.77896
13	CL(74:6)	1.77392
14	CL(80:13)	1.73457
15	CL(80:11)	1.73196
16	CL(76:4)	1.72409
17	CL(72:2)	1.70441
18	CL(72:6)	1.69483
19	CL(70:8)	1.69373
20	CL(76:8)	1.68624
21	CL(76:5)	1.65998
22	CL(76:9)	1.6501
23	CL(70:4)	1.64654
24	CL(80:12)	1.64309
25	CL(72:4)	1.64108

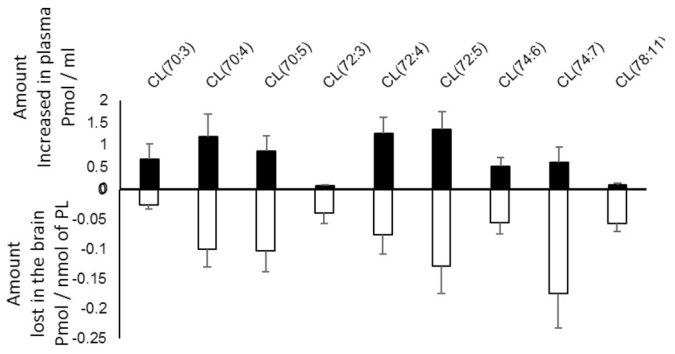

Fig. 4. Bar graph showing the changes in the amount of brain cardiolipins vs plasma cardiolipins after TBI. Values are Mean ± SD.

cortex. The essential requirement of lipids as building blocks of membranes, bio-energetic fuel, and signaling molecules has prompted the use of lipidomics analysis for discovering markers of human health and diseases. The brain is one of the most lipid-rich tissues, with a hallmark cardiolipinome of diverse species. We recently showed that these brain-type CL species accumulate in plasma at levels proportional to injury severity and correlate with functional outcome after global cerebral ischemia in adults (Anthonymuthu et al., 2019). Since CL is exclusively located in mitochondria, the identification of brain-type CLs in systemic circulation as a result of neurological injury may indicate underlying mitochondrial dysfunction/loss and could serve as a target for therapeutic intervention.

Since CLs are predominantly located in the inner mitochondrial membrane, one might wonder how they are released into plasma after CCI and also whether or not circulating CLs might have any signaling role. To date, two modes of intracellular signaling by CL are well established. First, translocation of CL from the inner mitochondrial membrane to the outer mitochondrial membrane and its subsequent oxidation through the cytochrome C/CL complex resulting in the release of pro-apoptotic signals into the cytoplasm. This, in turn, activates the caspase pathway which executes apoptotic cell death (Kagan et al., 2005a). Second, membrane externalization of CL alone can act as an "eat-me" signal via activation of the autophageal protein, microtubule-associated-protein-1 light chain 3 (LC3) (Chu et al., 2013). Although these two pathways are implicated in the pathogenesis of TBI, it is unlikely that apoptosis and autophagy would result in the release of CL into systemic circulation for several reasons: a) we have not identified any oxidized CL products in the plasma, and b) autophagy occurs intracellularly with the components of the cellular compartments degraded or reused within the cell (Kim and Lee, 2014). Alternatively, activation of regulated cell death pathways other than apoptosis may result in the release of mitochondrial fragments (Maeda and Fadeel, 2014). Mitochondrial-derived particles are a component of the inter-organelle communication and damage-associated molecular patterns (DAMPs) that aid in quality control of mitochondria (Sugiura et al., 2014). Recent studies revealed the presence of mitochondria-derived exosomes in blood after TBI (Goetzl et al., 2017). Furthermore, CL-exposed brain-derived mitochondrial microparticles were detected in the peripheral blood of mice after fluid percussion TBI (Zhao et al., 2016). The functional role of CLs in the peripheral circulation has been realized recently. In mice, CL-exposed microparticles contributed to TBI associated coagulopathy (Zhao et al., 2016). Moreover, plasma CLs were shown to play important roles in inflammation and immunity (Balasubramanian et al., 2015; Chakraborty et al., 2017). With strong evidence for a role for extracellular mitochondrial components in regulation of the immune response, it is possible that plasma CLs after TBI are not simply biomarkers, but play a role in the mediation and/or regulation of some facet of the inflammatory response to injury.

Brain not only posseses a complex lipidome but also contains many unique lipids. This makes brain lipids a vulnerable target for physiological changes as well as a potential messengers under such conditions. Many lipid-based biomarkers have been identified in chronic and acute neurological diseases. The brain contains about 80% of the body's 24(*S*)-hydroxycholesterol (24S-OHC), one of the oxidized derivatives of cholesterol (Lutjohann et al., 1996). 24S-OHC levels were also shown to increase in major neurodegenerative diseases such as Alzheimer's Disease, multiple sclerosis, Parkinson's disease and Huntington disease (Sun et al., 2016). Similarly, palmitic acid, stearic acid, oleic acid, α-linoleic acid, DHA (Chua et al., 2016), plasmalogens (Graham et al., 2018), several species of phosphatidylethanolamine, PC species (González-Domínguez et al., 2014), and lysophosphoinositol species (Mapstone et al., 2014) were reported as biomarkers for Alzheimer's disease and memory loss.

Traumatic brain injury is a heterogeneous disease in terms of both epidemiology and disease progression. This heterogeneity makes it difficult to asses the level of injury and prognosis. Conventional classification of TBI relies on neurological examination and imaging techniques. Though these modalities are routinely used in the clinical arena, there is a need for surrogate peripheral biomarkers, which can be used by themselves or in combination with the existing imaging modalities to assess the temporal course of secondary injury evolution and to assess treatment response after TBI. In line with this, several attempts have been made to identify lipid biomarkers in acute brain injury. Sheth et al., showed elevated levels of various sphingolipid species after CCI in adult rats and after middle cerebral artery occlusion in adult mice (Sheth et al., 2015). The sphingolipid score, a value derived from the sum of two elevated sphingolipid species, differentiated the animals exposed to stroke and was correlated with lesion volume (Sheth et al., 2015). Several studies in experimental TBI showed decreases in PUFA-containing phospholipids: PE, PC, and PI in plasma (Abdullah et al., 2014; Emmerich et al., 2015; Emmerich et al., 2017). In a military population with mild TBI, a significant reduction in both plasma monounsaturated fatty acid containing PC and PI species and the ratio of arachidonic acid to docosahexaenoic acid containing PC and PE lipids was observed (Emmerich et al., 2015). These studies, however, did not investigate plasma CL levels likely because of its low abundance and the requirement for newly developed high-resolution LC/MS-MS techniques that are used in this study.

Phospholipids account for 35–50% of total lipids in the brain. Many

phospholipids in the brain contain PUFAs in their sn-2 as well as sn-1 positions making them susceptible to oxidation after TBI (Anthonymuthu et al., 2018). Different phospholipases can hydrolyze non-oxidized (e.g., calcium-dependent cytosolic phospholipase A2 [PLA2]) or oxidized fatty acyl chains (e.g., calcium-independent mitochondrial PLA2,) after TBI (Anthonymuthu et al., 2016). Resulting products of non-oxidized or oxidized fatty acids, as well as lyso-phospholipids, have been shown to accumulate in the brain after experimental and clinical TBI (Anthonymuthu et al., 2017; Anthonymuthu et al., 2018). The primary products of phospholipid oxidation are hydroperoxy species. Their degradation products such as F2-isoprostanes were shown to be increased in the CSF of infants and children with severe TBI versus control samples and peaked at 1 day after injury (Bayir et al., 2002). This increase in F_2-isoprostane correlated with the significant reduction in antioxidant reserves: ascorbate and glutathione (Bayir et al., 2002). Although detection of end products of lipid oxidation can help with estimating the overall lipid peroxidation burden, these measures cannot identify the specific phospholipid(s) that undergo oxidation. The latter is important in providing mechanistic understanding and directing therapeutic targeting. Our previous studies have shown that CL undergoes cytochrome *c* mediated oxidation after CCI in PND17 rats. A CL-targeting nitroxide, XJB-5-131, attenuated CL oxidation and improved functional outcome in immature rats (Ji et al., 2012). Future studies evaluating plasma CL as a measure of therapeutic effectiveness of mitochondria-targeted nitroxides after TBI could be revealing.

To date, most of the biofluidic biomarkers identified after TBI are proteins such as S100β, neuron-specific enolase (NSE), myelin basic protein (MBP), Neurofilament heavy chain protein (NF-H), glial fibrillary acidic protein (GFAP), and ubiquitin C-terminal hydrolase-L1 (UCHL1) (Agoston and Shutes-David, 2017). Compared to the protein biomarkers, CL is smaller in size and more hydrophobic in nature. Therefore, CL can be easily released into the peripheral circulation after crossing the blood-brain barrier. Moreover, mitochondria-derived microparticles can transmigrate through the blood-brain barrier in a platelet-dependent manner (Tian et al., 2015).

In this study, we chose to utilize 17 day old rats. PND17 represents a time point of active synaptogenesis, analogous to the human toddler, and is also a critical time when mature synaptic function is being established (Semple et al., 2013). We and others have shown that diversity of CL species is similar between the mouse, rat and human brains (Anthonymuthu et al., 2019; Cheng et al., 2008). Cheng et al., reported that in the mouse cortex, CL levels significantly increased during the prenatal period, transiently decreased at birth, and then began to increase until PND40. Interestingly CLs containing shorter saturated fatty acid chains such as oleic acid (C18:1) and palmitic acid (C16:1) gradually decreased around the perinatal period and were replaced by CLs containing longer chain polyunsaturated fatty acids such as arachidonic acid (C20:4) and docosahexaenoic acid (C22:6), reaching the adult CL profile by PND30. There was no significant difference in total cortical CL levels between PND7 and PND15 mice, analogs to human newborn and toddler, respectively. The profile of brain CL was slightly different with lower C16:1 and higher C18:1 and C20:4 content in the PND17 vs. PND15 mouse cortex.

It has been increasingly recognized that the pathology and the outcome of TBI are sex-dependent (Bayir et al., 2004; Vagnerova et al., 2008). Experiments with the female rats or a mixed population might be required to extend these observations to the general population. However, previous studies suggest that gender-based differences will likely play a minor role in plasma CL levels and profile both under normal circumstances and after injury. For example, in our previous study, we did not observe sex differences in plasma CL profile between males and females in control and cardiac arrest patients (Anthonymuthu et al., 2019). Similarly, previous studies in male and female mice showed comparable CL content and saturation level in the cortex after post-natal day 4 in both sexes (Acaz-Fonseca et al., 2017).

In conclusion, using high-resolution LC-MS we showed that brain-type CL species increase in plasma after CCI in PND17 rats and this increase quantitatively correlates with their loss from the injured cortex suggesting a possible release of CLs from the brain into the plasma after TBI. The identification of brain-type CLs in systemic circulation as a result of neurological injury may indicate underlying mitochondrial dysfunction/loss and could serve as a target for therapeutic intervention. Future studies evaluating theranostic potential of plasma CL in experimental and clinical TBI are warranted.

Acknowledgments

Supported by NIH (HL114453, AI068021, NS076511, NS084604 and NS061817).

References

Abdullah, L., Evans, J.E., Ferguson, S., Mouzon, B., Montague, H., Reed, J., Crynen, G., Emmerich, T., Crocker, M., Pelot, R., Mullan, M., Crawford, F., 2014. Lipidomic analyses identify injury-specific phospholipid changes 3 mo after traumatic brain injury. FASEB J. 28, 5311–5321.

Acaz-Fonseca, E., Ortiz-Rodriguez, A., Lopez-Rodriguez, A.B., Garcia-Segura, L.M., Astiz, M., 2017. Developmental sex differences in the metabolism of Cardiolipin in mouse cerebral cortex mitochondria. Sci. Rep. 7, 43878.

Agoston, D.V., Shutes-David, A., 2017. Biofluid biomarkers of traumatic brain injury. Brain Inj. 31, 1195–1203.

Anthonymuthu, T.S., Kenny, E.M., Bayır, H., 2016. Therapies targeting lipid peroxidation in traumatic brain injury. Brain Res. 1640, 57–76.

Anthonymuthu, T.S., Kenny, E.M., Amoscato, A.A., Lewis, J., Kochanek, P.M., Kagan, V.E., Bayır, H., 2017. Global assessment of oxidized free fatty acids in brain reveals an enzymatic predominance to oxidative signaling after trauma. Biochim. Biophys. Acta (BBA) - Mol. Basis Dis. 1863, 2601–2613.

Anthonymuthu, T.S., Kenny, E.M., Lamade, A.M., Kagan, V.E., Bayır, H., 2018. Oxidized phospholipid signaling in traumatic brain injury. Free Radic. Biol. Med. 124, 493–503.

Anthonymuthu, T.S., Kenny, E.M., Lamade, A.M., Gidwani, H., Krehel, N.M., Misse, A., Gao, X., Amoscato, A.A., Straub, A.C., Kagan, V.E., Dezfulian, C., Bayir, H., 2019. Lipidomics detection of brain cardiolipins in plasma is associated with outcome after cardiac arrest. Crit. Care Med. 47 (4), e292–e300.

Asemota, A.O., George, B.P., Bowman, S.M., Haider, A.H., Schneider, E.B., 2013. Causes and trends in traumatic brain injury for United States adolescents. J. Neurotrauma 30, 67–75.

Balasubramanian, K., Maeda, A., Lee, J.S., Mohammadyani, D., Dar, H.H., Jiang, J.F., St Croix, C.M., Watkins, S., Tyurin, V.A., Tyurina, Y.Y., Kloditz, K., Polimova, A., Kapralova, V.I., Xiong, Z., Ray, P., Klein-Seetharaman, J., Mallampalli, R.K., Bayir, H., Fadeel, B., Kagan, V.E., 2015. Dichotomous roles for externalized cardiolipin in extracellular signaling: promotion of phagocytosis and attenuation of innate immunity. Sci. Signal. 8, ra95.

Bayir, H., Kagan, V.E., Tyurina, Y.Y., Tyurin, V., Ruppel, R.A., Adelson, P.D., Graham, S.H., Janesko, K., Clark, R.S.B., Kochanek, P.M., 2002. Assessment of antioxidant reserves and oxidative stress in cerebrospinal fluid after severe traumatic brain injury in infants and children. Pediatr. Res. 51, 571.

Bayir, H., Marion, D.W., Puccio, A.M., Wisniewski, S.R., Janesko, K.L., Clark, R.S., Kochanek, P.M., 2004. Marked gender effect on lipid peroxidation after severe traumatic brain injury in adult patients. J. Neurotrauma 21, 1–8.

Bayir, H., Tyurin, V.A., Tyurina, Y.Y., Viner, R., Ritov, V., Amoscato, A.A., Zhao, Q., Zhang, X.J., Janesko-Feldman, K.L., Alexander, H., Basova, L.V., Clark, R.S.B., Kochanek, P.M., Kagan, V.E., 2007. Selective early cardiolipin peroxidation after traumatic brain injury: an oxidative lipidomics analysis. Annals Neurol. 62, 154–169.

Chakraborty, K., Raundhal, M., Chen, B.B., Morse, C., Tyurina, Y.Y., Khare, A., Oriss, T.B., Huff, R., Lee, J.S., St Croix, C.M., Watkins, S., Mallampalli, R.K., Kagan, V.E., Ray, A., Ray, P., 2017. The Mito-DAMP cardiolipin blocks IL-10 production causing persistent inflammation during bacterial pneumonia. Nat. Commun. 8, 13944.

Chao, H., Anthonymuthu, T.S., Kenny, E.M., Amoscato, A.A., Cole, L.K., Hatch, G.M., Ji, J., Kagan, V.E., Bayır, H., 2018. Disentangling oxidation/hydrolysis reactions of brain mitochondrial cardiolipins in pathogenesis of traumatic injury. JCI Insight 3, e97677.

Cheng, H., Mancuso, D.J., Jiang, X., Guan, S., Yang, J., Yang, K., Sun, G., Gross, R.W., Han, X., 2008. Shotgun lipidomics reveals the temporally dependent, highly diversified cardiolipin profile in the mammalian brain: temporally coordinated post-natal diversification of cardiolipin molecular species with neuronal remodeling. Biochemistry 47, 5869–5880.

Chu, C.T., Ji, J., Dagda, R.K., Jiang, J.F., Tyurina, Y.Y., Kapralov, A.A., Tyurin, V.A., Yanamala, N., Shrivastava, I.H., Mohammadyani, D., Wang, K.Z.Q., Zhu, J., Klein-Seetharaman, J., Balasubramanian, K., Amoscato, A.A., Borisenko, G., Huang, Z., Gusdon, A.M., Cheikhi, A., Steer, E.K., Wang, R., Baty, C., Watkins, S., Bahar, I., Bayir, H., Kagan, V.E., 2013. Cardiolipin externalization to the outer mitochondrial membrane acts as an elimination signal for mitophagy in neuronal cells. Nat. Cell Biol. 15, 1197–1205.

Chua, E.W., Cree, S.L., Ton, K.N., Lehnert, K., Shepherd, P., Helsby, N., Kennedy, M.A., 2016. Cross-comparison of exome analysis, next-generation sequencing of amplicons,

and the iPLEX((R)) ADME PGx panel for pharmacogenomic profiling. Front. Pharmacol. 7, 1.
Dewan, M.C., Mummareddy, N., Wellons, J.C., Bonfield, C.M., 2016. Epidemiology of global pediatric traumatic brain injury: qualitative review. World Neurosurg. 91, 497–509 (e491).
Emmerich, T., Abdullah, L., Crynen, G., Dretsch, M., Evans, J., Ait-Ghezala, G., Reed, J., Montague, H., Chaytow, H., Mathura, V., Martin, J., Pelot, R., Ferguson, S., Bishop, A., Phillips, J., Mullan, M., Crawford, F., 2015. Plasma Lipidomic profiling in a military population of mild traumatic brain injury and post-traumatic stress disorder with Apolipoprotein E ε4–dependent effect. J. Neurotrauma 33, 1331–1348.
Emmerich, T., Abdullah, L., Ojo, J., Mouzon, B., Nguyen, T., Laco, G.S., Crynen, G., Evans, J.E., Reed, J., Mullan, M., Crawford, F., 2017. Mild TBI results in a long-term decrease in circulating phospholipids in a mouse model of injury. NeuroMolecular Med. 19, 122–135.
Goetzl, L., Merabova, N., Darbinian, N., Martirosyan, D., Poletto, E., Fugarolas, K., Menkiti, O., 2017. Diagnostic potential of neural exosome cargo as biomarkers for acute brain injury. Ann. Clin. Transl. Neurol. 5, 4–10.
González-Domínguez, R., García-Barrera, T., Gómez-Ariza, J.L., 2014. Combination of metabolomic and phospholipid-profiling approaches for the study of Alzheimer's disease. J. Proteome 104, 37–47.
Graham, E.M., Everett, A.D., Delpech, J.C., Northington, F.J., 2018. Blood biomarkers for evaluation of perinatal encephalopathy: state of the art. Curr. Opin. Pediatr. 30, 199–203.
Ji, J., Kline, A.E., Amoscato, A., Samhan-Arias, A.K., Sparvero, L.J., Tyurin, V.A., Tyurina, Y.Y., Fink, B., Manole, M.D., Puccio, A.M., Okonkwo, D.O., Cheng, J.P., Alexander, H., Clark, R.S., Kochanek, P.M., Wipf, P., Kagan, V.E., Bayir, H., 2012. Lipidomics identifies cardiolipin oxidation as a mitochondrial target for redox therapy of brain injury. Nat. Neurosci. 15, 1407–1413.
Kagan, V.E., Tyurin, V.A., Jiang, J., Tyurina, Y.Y., Ritov, V.B., Amoscato, A.A., Osipov, A.N., Belikova, N.A., Kapralov, A.A., Kini, V., 2005a. Cytochrome c acts as a cardiolipin oxygenase required for release of proapoptotic factors. Nat. Chem. Biol. 1, 223.
Kagan, V.E., Tyurin, V.A., Jiang, J., Tyurina, Y.Y., Ritov, V.B., Amoscato, A.A., Osipov, A.N., Belikova, N.A., Kapralov, A.A., Kini, V., Vlasova, I.I., Zhao, Q., Zou, M., Di, P., Svistunenko, D.A., Kurnikov, I.V., Borisenko, G.G., 2005b. Cytochrome c acts as a cardiolipin oxygenase required for release of proapoptotic factors. Nat. Chem. Biol. 1, 223–232.
Kagan, V.E., Tyurina, Y.Y., Tyurin, V.A., Mohammadyani, D., Angeli, J.P., Baranov, S.V., Klein-Seetharaman, J., Friedlander, R.M., Mallampalli, R.K., Conrad, M., Bayir, H., 2015. Cardiolipin signaling mechanisms: collapse of asymmetry and oxidation. Antioxid. Redox Signal. 22, 1667–1680.
Kilbaugh, T.J., Karlsson, M., Duhaime, A.C., Hansson, M.J., Elmer, E., Margulies, S.S., 2016. Mitochondrial response in a toddler-aged swine model following diffuse non-impact traumatic brain injury. Mitochondrion 26, 19–25.
Kim, K.H., Lee, M.S., 2014. Autophagy–a key player in cellular and body metabolism. Nat. Rev. Endocrinol. 10, 322–337.
Kochanek, P.M., Carney, N., Adelson, P.D., Ashwal, S., Bell, M.J., Bratton, S., Carson, S., Chesnut, R.M., Ghajar, J., Goldstein, B., Grant, G.A., Kissoon, N., Peterson, K., Selden, N.R., Tasker, R.C., Tong, K.A., Vavilala, M.S., Wainwright, M.S., Warden, C.R., 2012. Guidelines for the acute medical management of severe traumatic brain injury in infants, children, and adolescents–second edition. Pediatr. Crit. Care Med. 13 (Suppl. 1), S1–82.
Liu, G.Y., Moon, S.H., Jenkins, C.M., Li, M., Sims, H.F., Guan, S., Gross, R.W., 2017. The phospholipase iPLA2gamma is a major mediator releasing oxidized aliphatic chains from cardiolipin, integrating mitochondrial bioenergetics and signaling. J. Biol. Chem. 292, 10672–10684.
Lutjohann, D., Breuer, O., Ahlborg, G., Nennesmo, I., Siden, A., Diczfalusy, U., Bjorkhem, I., 1996. Cholesterol homeostasis in human brain: evidence for an age-dependent flux of 24S-hydroxycholesterol from the brain into the circulation. Proc. Natl. Acad. Sci. U. S. A. 93, 9799–9804.
Maeda, A., Fadeel, B., 2014. Mitochondria released by cells undergoing TNF-[alpha]-induced necroptosis act as danger signals. Cell Death Dis. 5, e1312.
Mapstone, M., Cheema, A.K., Fiandaca, M.S., Zhong, X., Mhyre, T.R., MacArthur, L.H., Hall, W.J., Fisher, S.G., Peterson, D.R., Haley, J.M., Nazar, M.D., Rich, S.A., Berlau, D.J., Peltz, C.B., Tan, M.T., Kawas, C.H., Federoff, H.J., 2014. Plasma phospholipids identify antecedent memory impairment in older adults. Nat. Med. 20, 415.
Pfeiffer, K., Gohil, V., Stuart, R.A., Hunte, C., Brandt, U., Greenberg, M.L., Schagger, H., 2003. Cardiolipin stabilizes respiratory chain supercomplexes. J. Biol. Chem. 278, 52873–52880.
Robertson, C.L., Saraswati, M., 2015. Progesterone protects mitochondrial function in a rat model of pediatric traumatic brain injury. J. Bioenerg. Biomembr. 47, 43–51.
Robertson, C.L., Scafidi, S., McKenna, M.C., Fiskum, G., 2009. Mitochondrial mechanisms of cell death and neuroprotection in pediatric ischemic and traumatic brain injury. Exp. Neurol. 218, 371–380.
Semple, B.D., Blomgren, K., Gimlin, K., Ferriero, D.M., Noble-Haeusslein, L.J., 2013. Brain development in rodents and humans: identifying benchmarks of maturation and vulnerability to injury across species. Prog. Neurobiol. 106-107, 1–16.
Sheth, S.A., Iavarone, A.T., Liebeskind, D.S., Won, S.J., Swanson, R.A., 2015. Targeted lipid profiling discovers plasma biomarkers of acute brain injury. PLoS One 10, e0129735.
Singh, I.N., Sullivan, P.G., Deng, Y., Mbye, L.H., Hall, E.D., 2006. Time course of post-traumatic mitochondrial oxidative damage and dysfunction in a mouse model of focal traumatic brain injury: implications for neuroprotective therapy. J. Cereb. Blood Flow Metab. 26, 1407–1418.
Stovell, M.G., Mada, M.O., Helmy, A., Carpenter, T.A., Thelin, E.P., Yan, J.-L., Guilfoyle, M.R., Jalloh, I., Howe, D.J., Grice, P., Mason, A., Giorgi-Coll, S., Gallagher, C.N., Murphy, M.P., Menon, D.K., Hutchinson, P.J., Carpenter, K.L.H., 2018. The effect of succinate on brain NADH/NAD+ redox state and high energy phosphate metabolism in acute traumatic brain injury. Sci. Rep. 8, 11140.
Sugiura, A., McLelland, G.L., Fon, E.A., McBride, H.M., 2014. A new pathway for mitochondrial quality control: mitochondrial-derived vesicles. EMBO J. 33, 2142–2156.
Sun, M.-Y., Linsenbardt, A.J., Emnett, C.M., Eisenman, L.N., Izumi, Y., Zorumski, C.F., Mennerick, S., 2016. 24(S)-Hydroxycholesterol as a modulator of neuronal Signaling and survival. Neuroscientist 22, 132–144.
Tian, Y., Salsbery, B., Wang, M., Yuan, H., Yang, J., Zhao, Z., Wu, X., Zhang, Y., Konkle, B.A., Thiagarajan, P., Li, M., Zhang, J., Dong, J.-f., 2015. Brain-derived microparticles induce systemic coagulation in a murine model of traumatic brain injury. Blood 125, 2151.
Tilford, J.M., Aitken, M.E., Anand, K.J., Green, J.W., Goodman, A.C., Parker, J.G., Killingsworth, J.B., Fiser, D.H., Adelson, P.D., 2005. Hospitalizations for critically ill children with traumatic brain injuries: a longitudinal analysis. Crit. Care Med. 33, 2074–2081.
Tyurina, Y.Y., Poloyac, S.M., Tyurin, V.A., Kapralov, A.A., Jiang, J., Anthonymuthu, T.S., Kapralova, V.I., Vikulina, A.S., Jung, M.-Y., Epperly, M.W., Mohammadyani, D., Klein-Seetharaman, J., Jackson, T.C., Kochanek, P.M., Pitt, B.R., Greenberger, J.S., Vladimirov, Y.A., Bayır, H., Kagan, V.E., 2014. A mitochondrial pathway for biosynthesis of lipid mediators. Nat. Chem. 6, 542.
Vagnerova, K., Koerner, I.P., Hurn, P.D., 2008. Gender and the injured brain. Anesth. Analg. 107, 201–214.
You, Z., Savitz, S.I., Yang, J., Degterev, A., Yuan, J., Cuny, G.D., Moskowitz, M.A., Whalen, M.J., 2008. Necrostatin-1 reduces histopathology and improves functional outcome after controlled cortical impact in mice. J. Cereb. Blood Flow Metab. 28, 1564–1573.
Zhao, Z., Wang, M., Tian, Y., Hilton, T., Salsbery, B., Zhou, E.Z., Wu, X., Thiagarajan, P., Boilard, E., Li, M., Zhang, J., Dong, J.F., 2016. Cardiolipin-mediated procoagulant activity of mitochondria contributes to traumatic brain injury-associated coagulopathy in mice. Blood 127, 2763–2772.